NRC Research Press

ARTICLE

Branched-chain and dendritic lipids for nanoparticles

Michael W. Meanwell, Connor O'Sullivan, Perry Howard, and Thomas M. Fyles

Abstract: Lipid nanoparticles (LNPs) for drug-delivery applications are largely derived from natural lipids. Synthetic lipids, particularly those incorporating branched hydrocarbons and hyper-branched hydrocarbon architectures, may afford enhanced lipophilicity with enhanced fluidity and thereby lead to LNP stabilization. Hydrocarbon anchors based on serinol diesters were prepared from linear C_n (n = 14, 16, 18) and branched (n = 16) acids with Boc-protected serinol. These diesters were further dimerized on an iminodiacetamide backbone to provide eight branched-chain and dendritic lipid anchors. Derivatization of these core structures provided eight PEG-lipids and seven thiopurine linked lipid–drug conjugates. LNPs were prepared by microfluidic mixing from mixed lipids in ethanol diluted into aqueous media. The lipid–drug conjugates incorporated 5 mol% of a phosphocholine and 5 mol% of a commercial PEG-lipid to form LNPs with a thiopurine drug loading of 15 wt%. The PEG–lipids prepared were formulated at 1.5 mol% as a surface stabilizer to LNPs containing dsDNA lipoplexes. The stability of the LNPs was assessed under different storage conditions through monitoring of particle size. For both LNPs from lipid–thiopurine conjugates and the PEG-lipid systems, there is strong preliminary evidence that hydrocarbon branching results in LNP stabilization. Four of the lipid–drug conjugate formulations were stable to cell culture conditions (10% serum, 37 °C) and the toxicity of these LNPs was assessed in two cell lines relative to the free thiopurines in the medium. The observed toxicity is consistent with cellular uptake of the LNPs and reductive release of the cargo thiopurine within the cell.

Key words: lipid synthesis, PEG-lipid, lipid–drug conjugate, electrospray mass spectrometry, lipid nanoparticle stability.

Résumé : Les nanoparticules de lipides (NPL) dans les applications d'administration des médicaments sont largement dérivées de lipides naturels. Or, des lipides synthétiques, en particulier ceux qui comporteraient des chaînes d'hydrocarbures ramifiées ou des architectures d'hydrocarbures hyper-ramifiées, pourraient présenter une lipophilie et une fluidité accrues, et ainsi permettre la stabilisation des NPL. Nous avons synthétisé des diesters de sérinol comme points d'ancrage pour les hydrocarbures à partir d'acides linéaires C_n (n = 14, 16, 18) et ramifiés (n = 16) et de sérinol protégé par Boc. Nous avons par la suite formé un dimère de ces diesters sur un squelette d'iminodiacétamide pour produire huit composés à ancrages lipidiques de structure ramifiée ou dendritique. La dérivation de ces structures de base a produit huit lipides liés au PEG et sept conjugués lipide–médicament liés à la thiopurine. Nous avons synthétisé les NPL par mélange microfluide à partir de lipides mélangés dans l'éthanol puis dilués en milieu aqueux. Les conjugués lipide–médicament ont incorporé 5 mol % de phosphocholine et 5 mol % d'un lipide lié au PEG vendu sur le marché pour former les NPL dont la charge du médicament lié à la thiopurine était de 15 % p/p. Les lipides liés au PEG que nous avons synthétisés ont été mis en formule à 1,5 mol % comme stabilisant de surface des NPL contenant des lipoplexes d'ADN bicaténaire. Nous avons évalué la stabilité des NPL dans différentes conditions d'entreposage en mesurant la taille des particules. Dans le cas des NPL à base de conjugués lipides-thiopurine comme dans celui des systèmes de lipides liés au PEG, les résultats préliminaires appuient fortement l'hypothèse selon laquelle la ramification des chaînes d'hydrocarbures permet de stabiliser les NPL. En effet, quatre des préparations de conjugué lipide–médicament étaient stables en conditions de culture cellulaire (sérum à 10 %, 37 °C). En outre, nous avons évalué la toxicité de ces NPL dans deux lignées cellulaires comparativement à celle de thiopurines libres dans le milieu. La toxicité observée est cohérente avec l'absorption des NPL par la cellule et la libération réductrice de la charge de thiopurine dans la cellule. [Traduit par la Rédaction]

Mots-clés : synthèse des lipides, lipide lié au PEG, conjugué lipide–médicament, spectrométrie de masse à ionisation par électronébulisateur, stabilité des nanoparticules de lipides.

Introduction

Lipid nanoparticles (LNPs) are an emerging drug delivery strategy in biomedical research and therapy.[1–5] LNPs consist of a condensed lipidic core — solid, nanostructured, and (or) fluid — with a hydrophilic outer layer that may bear additional functionality. The drug loading in the particle can be noncovalent, as in the electrostatic complexes (lipoplexes) of plasmid DNA or siRNA with cationic lipids,[6,7] or covalent, as in the so-called lipid–drug conjugates (LDCs) in which a hydrophilic drug is linked as a prodrug to a lipid via a functionality that can be metabolically cleaved in the target cell.[3,8,9] The ultimate utility of a particular LNP is based on an array of formulation variables — lipid composition and proportion, drug loading, surface modifying agents, and mixing parameters — that control particle size, lifetime in biological media, and cellular uptake.[3] The formulation space appears to be vast and, yet, is predominantly based on a relatively restricted set of naturally derived phospholipids possessing two fatty acid chains of C_{16}–C_{18} as glycerol diesters. Although this may limit the potential toxicity of the LNP, it also imposes geometrical restraints[10] on the packing of lipids and the overall stability of the LNP.

Received 30 August 2016. Accepted 28 October 2016.

M.W. Meanwell and T.M. Fyles. Department of Chemistry, University of Victoria, Victoria, BC V8W 3V6, Canada.
C. O'Sullivan and P. Howard. Department of Biochemistry and Microbiology, University of Victoria, Victoria, BC V8P 5C2, Canada.
Corresponding author: Thomas M. Fyles (email: tmf@uvic.ca).

Scheme 1. Branched-chain and dendritic lipid designs.

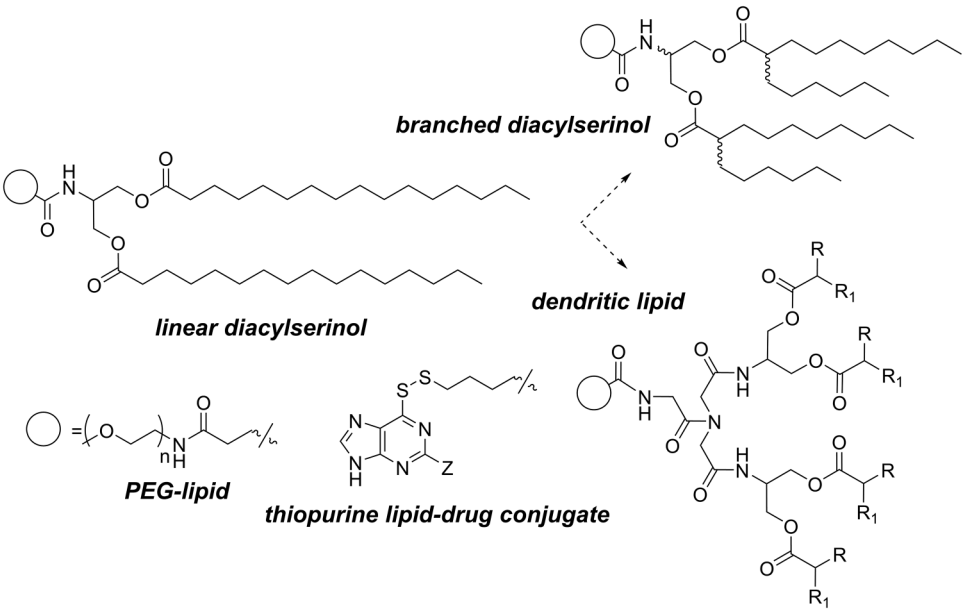

Specific lipids within LNP formulations are designed to perform specialized functions. For example, poly (ethylene glycol)-derivatized lipids (PEG-lipids) are used to reduce nonspecific protein binding by the LNP surface and thereby increase the lifetime of LNPs in serum.[2,11,12] Current commercially available PEG-lipids (usually diC_{18}) insufficiently anchor the polymer to the LNP, limiting both storage lifetime and circulation times and leading to immunogenic activity; these effects may be linked to hydrolysis of esters within the PEG-lipid,[13] but PEG-lipid loss to the medium is also implicated.[14] PEG anchoring can be compared with the anchoring of oligosaccharides to cell surfaces achieved in nature by lipid A — a disaccharide bearing up to six branched fatty acid chains.[15] Lipid A anchors invest nearly twice the hydrocarbon, incorporated as shorter branched chains, to anchor the hydrophilic surface oligosaccharide relative to a comparable PEG-lipid.

Naturally derived lipids may also be similarly poor as the core structures for the formation of LDC nanoparticles. Typically, a hydrophilic drug is conjugated as the head group of a diacylglycerol. Hydrophobic self-assembly is expected to immobilize the LDC into a LNP. To achieve high drug or particle loading and thereby reduce side effects, the hydrophobic component must be as small as possible relative to the drug head group.[3] The inherent shape of a diacylglycerol tends towards a lamellar lipid arrangement[10] that will inhibit the formation of closed LNPs structures. Even if formed, the specific chain packing of a natural diacylglycerol may compromise particle integrity even with sufficient hydrocarbon present to drive the self-assembly of the LNP.

Lipid self-assembly into LNPs and other lipid morphologies is a dynamic balance between lipid shape, charge, and hydrophobicity.[10] Many successful formulations, particularly for the formation of LNPs with solid cores, are based on lipid mixtures of glycerol diesters, neutral glycerol triesters and other harder fats, and fluidizing glycerol monoesters along with surfactants to stabilize the particle surface.[16] Engineering lipid mixtures in this context not only is equivalent to adjusting the average lipid shape and charge to control overall LNP size and charge, but also leads to complex phase behavior and phase separation and potentially to compromised LNP stability and performance.[16]

As naturally derived lipids provide only limited diversity of component shapes and charges, we recognized an opportunity to explore synthetic lipids as a route to access a wider range of these key properties. Inspired by the reliance of lipid A on shorter branched chains to anchor surface oligosaccharides, we initially focussed on designs incorporating branched hydrocarbon chains that are available commercially as Guerbet-derived acids.[17,18] We subsequently realized that branching could also be achieved with dendrimer-like dimerization on an imino-diacetamide backbone (Scheme 1). The latter structures are the hydrophobic inverse of lipids bearing dendritic head groups.[19,20] Branching, shorter chains, and chain multiplicity all are expected to reduce the crystallinity of the hydrocarbon and enhance the miscibility of the chains with other components.

Our focus here is on serinol diesters of fatty acids[21] that offer the potential to explore alternative hydrocarbon anchoring topologies and their consequences for LNP formation and stability as either PEG-lipid anchors or as the driving components of LDC nanoparticle formation. Serinol substructures occur in sphingolipids[22] and serinolipids,[23–26] but it is usually the amine, not the hydroxyl group, that is acylated. Serinol-derived diesters, with linear C_{14}–C_{18} chains bearing (poly) ammonium head groups, are widely reported as transfection reagents.[27–31]

The goal of this initial study is to develop the synthesis and characterization of the core lipids and simple derivatives for the formulation of LNPs and to uncover if hydrocarbon chain branching affords any advantages in LNP stabilization. As shown in Scheme 1, we focussed on a PEG-lipid derivative and a thiopurine lipid–drug conjugate as initial targets.

PEG-lipids play a number of roles in both the formulation and circulation stability of LNPs. When formulating LNPs, the PEG surface coating prevents aggregation and contributes to obtaining stable, small, and mono-disperse nanoparticles.[12,13] While providing a steric barrier to protect the LNP, the PEG also serves to significantly decrease the surface charge. This combination of steric barrier and reduced surface charge is generally assumed to prevent the LNPs from associating with serum proteins and ultimately leads to extended circulation times compared with their nonpegylated counterparts.[13,32] We anticipated some differential between branched-chain and linear isomers with respect to particle size stability if there is underlying merit to this lipid core design.

Thiopurines are frontline drugs in the treatment of childhood acute lymphoblastic leukaemia[33] and are widely used as immunosuppressants in the treatment of autoimmune disorders (e.g., Crohn's disease, rheumatoid arthritis) and as anti-rejection agents

in organ transplant patients.[34,35] The thiopurines are activated by a phosphoribosyl transferase to produce thiopurine nucleotide triphosphates (TTP), which are incorporated into DNA[34] causing mitotic death due to DNA damage.[36] The cytosol of most tumour cells is more reducing than in normal cells due to elevated free thiol/glutathione levels, and this tumour cell-specific reactivity has been exploited for tumour targeting, imaging, and drug delivery.[8,9,37–39] Accordingly, we incorporated a disulfide linkage to release the drug in tumorigenic cell lines with elevated reducing potential in the cytosol. In these initial studies, we were concerned with two issues: LNP particle size stability in storage and cell culture conditions and LNP uptake into suitable cells with reductive release of the drug.

Here, we report the synthesis of straight-chain, branched, and dendritic lipid anchors derivatized as both PEG-lipids and thiopurine lipid–drug conjugates. Experiments to monitor the particle-size stability of LNP formulations containing these lipids established that chain branching enhances LNP stability. Cell culture bioassays of LDC activity are consistent with LNP uptake and reductive thiopurine release from the LDCs.

Experimental

Synthetic procedures

General procedure for G1 lipid anchor synthesis

In a round-bottom flask, a stirred solution of thionyl chloride (10.0 equiv.) and **1a–1d** (1.0 equiv.) was refluxed for 2 h under a $CaSO_4$ drying tube. The reaction was monitored by ^{1}H NMR analysis of aliquots. The reaction was allowed to cool, and subsequently, the thionyl chloride was removed under vacuum on a rotary evaporator to obtain the acid chloride. In a round-bottom flask, **2** (1.0 equiv.) was dissolved in pyridine (10.0 equiv.) and the acid chloride (2.5 equiv.) was added dropwise. The mixture was then heated to 70 °C and left to stir for 3 h under a $CaSO_4$ drying tube. The reaction was monitored by ^{1}H NMR analysis of aliquots. Once completed, the reaction was cooled and diluted with DCM. The solution was then washed three times with 1 mol/L HCl and three times with 1 mol/L NaOH. The organic layer was then dried over anhydrous sodium sulfate and then gravity filtered. The solvent was removed under vacuum to obtain the Boc-protected anchor. Excess TFA was added dropwise to the Boc-protected anchor in a round-bottom flask. The reaction was left stirring for 1 h at room temperature and was monitored by TLC (silica gel, EtOAc/Hexanes as eluent, visualized by $KMnO_4$). Following completion of the reaction, TFA was removed on a rotary evaporator. NaOH (1 mol/L) was then added and **3a–3d** was extracted with DCM and washed three times with 1 mol/L NaOH. The organic layer was dried with anhydrous sodium carbonate and subsequently gravity filtered. DCM was removed on a rotary evaporator yielding **3a–3d**. No chromatography was necessary.

3a

By the general procedure: step 1, thionyl chloride (6.35 mL, 87.6 mmol) and **1a** (2.000 g, 8.757 mmol); step 2, **2** (0.596 g, 3.13 mmol) in pyridine (2.53 mL, 31.3 mmol) and the acid chloride (1.931 g, 7.835 mmol); step 3, TFA (5 mL) and the product of step 2; a waxy yellow solid was afforded in a 66% yield (1.06 g). ^{1}H NMR (300 MHz, $CDCl_3$) δ: 4.07 (m, 2H), 4.05 (m, 2H), 3.28 (m, 1H), 2.33 (t, 4H, 7.7 Hz), 1.62 (m, 4H), 1.48 (s(br), 2H), 1.26 (s, 40H), 0.88 (t, 6H, 7.0 Hz). ^{13}C NMR (75 MHz, $CDCl_3$): 173.6, 65.8, 49.3, 34.2, 31.9, 29.6, 29.6, 20.4, 29.3, 29.2, 29.1, 24.9, 22.7, 14.1. MS ((+) ESI): calcd for $C_{31}H_{62}NO_4^+$, 512.47 amu; found, 512.33 amu.

3b

By the general procedure: step 1, thionyl chloride (5.61 mL, 78.0 mmol) and **1b** (2.000 g, 7.800 mmol); step 2, **2** (0.558 g, 2.92 mmol) in pyridine (2.31 mL, 29.2 mmol) and the acid chloride (2.000 g, 7.299 mmol); step 3, TFA (5 mL) and the product of step 2; a waxy white solid was afforded in a 73% yield (1.21 g). ^{1}H NMR (300 MHz, $CDCl_3$) δ: 4.06 (m, 2H), 4.05 (m, 2H), 3.28 (m, 1H), 2.32 (t, 4H, J = 7.8 Hz), 1.61 (m, 4H), 1.24 (s, 48H), 0.87 (t, 6H). ^{13}C NMR (75 MHz, $CDCl_3$) δ: 173.8, 66.0, 49.5, 34.4, 32.1, 29.9, 29.9, 29.8, 29.7, 29.6, 29.5, 29.4, 25.2, 22.9, 14.3. MS ((+) ESI): calcd for $C_{35}H_{70}NO_4^+$, 568.53 amu; found, 568.33 amu.

3c

By the general procedure: step 1, thionyl chloride (5.66 mL, 78.2 mmol) and **1c** (2.30 mL, 7.82 mmol); step 2, **2** (0.488 g, 2.55 mmol) in pyridine (2.46 mL, 30.6 mmol) and the acid chloride (2.10 g, 7.64 mmol); step 3, TFA (5 mL) and the product of step 2; a light yellow oil was afforded in a 75% yield (1.09 g). ^{1}H NMR (300 MHz, $CDCl_3$) δ: 4.06 (m, 2H), 4.04 (m, 2H), 3.26 (m, 1 H), 2.34 (m, 2 H), 1.57, 1.44 (m, 8 H), 1.24 (s, 40 H), 0.86 (t, 12 H, J = 7.0 Hz). ^{13}C NMR (75 MHz, $CDCl_3$): 176.2, 65.5, 53.4, 49.4, 45.7, 32.4, 31.8, 31.6, 29.5, 29.4, 29.2, 29.2, 27.4, 27.4, 22.6, 22.6, 14.0, 14.0. MS ((+) ESI): calcd for $C_{35}H_{70}NO_4^+$, 568.53 amu; obtained, 568.33 amu.

3d

By the general procedure: step 1, thionyl chloride (5.10 mL, 70.3 mmol) and **1d** (2.000 g, 7.030 mmol); step 2, **2** (0.510 g, 2.67 mmol) in pyridine (2.15 mL, 26.7 mmol) and the acid chloride (2.020 g, 6.668 mmol); step 3, TFA (5 mL) and the product of step 2; a waxy white solid was afforded in a 67% yield (1.09 g). ^{1}H NMR (300 MHz, $CDCl_3$) δ: 4.09 (m, 2H), 4.07 (m, 2H), 3.30 (m, 1H), 2.34 (t, 4H, J = 7.5 Hz), 1.63 (m, 4H), 1.26 (s, 56H), 0.89 (t, 6H, J = 6.8 Hz). ^{13}C NMR (75 MHz, $CDCl_3$) δ: 173.8, 65.8, 49.6, 34.4, 32.1, 29.9, 29.9, 29.8, 29.7, 29.6, 29.5, 29.4, 25.2, 22.9, 14.3. MS ((+) ESI): calcd for $C_{39}H_{78}NO_4^+$, 624.59 amu; obtained, 624.53 amu.

General procedure — G2 lipid anchor synthesis — preparation of 5a–5d and 6a–6d

In a round-bottom flask, **4** (1 equiv.) was dissolved in dry DCM/DMF (1:1; 10 mmol/L). HBTU (2.4 equiv.), **3a–3d** (2.2 equiv.), and triethylamine (4.0 equiv.) were subsequently added. The solution was stirred for 20 h at room temperature and was monitored by ^{1}H NMR. Once completed, the reaction solution was diluted with EtOAc and washed three times with 1 mol/L HCl and three times with H_2O. The organic layer was then dried over anhydrous sodium sulfate, followed by gravity filtration. EtOAc and DCM were rotary evaporated to yield a Boc-protected product. Excess TFA was added dropwise to the Boc-protected product in a round-bottom flask. The reaction was left to stir for 1 h and monitored by ^{1}H NMR. Following completion of the reaction, TFA was removed on rotary evaporator and 1 mol/L NaOH was added to the round-bottom flask; then, the mixture was extracted with DCM and washed three times with 1 mol/L NaOH. The organic layer was then dried over sodium carbonate, followed by gravity filtration. DCM was removed on a rotary evaporator and **5a–5d** was isolated. The crude product was directly characterized; no purification was necessary (characterization: ^{1}H NMR, ^{13}C NMR, ESI–MS). In a round-bottom flask, Boc-glycine (1.1 equiv.) was dissolved in dry DCM/DMF (1:1; 10 mmol/L). To this, HOBt (1.2 equiv.), HBTU (1.2 equiv.), **5a–5d** (1.0 equiv.), and triethylamine (3.0 equiv.) were then added, and the resulting solution was left stirring at room temperature for 20 h. When the reaction was complete, monitored by ^{1}H NMR, the reaction solution was diluted with EtOAc and washed once with 1 mol/L HCl and three times with H_2O. The organic layer was then dried over anhydrous sodium sulfate and then gravity filtered. DCM and EtOAc were removed by rotary evaporation to yield a crude Boc-protected. Excess TFA was added in a round-bottom flask, and the reaction was left for 1 h. Following completion, as monitored by ^{1}H NMR, TFA was removed on a rotary evaporator. NaOH (1 mol/L) was added to convert to the amine and the glycine amide (**6a–6d**) was extracted with diethyl ether and subsequently washed three times with 1 mol/L NaOH. The organic layer was dried with anhydrous sodium carbonate

and then gravity filtered. Diethyl ether was removed to obtain the crude product, which was utilized without further purification.

5a *and* **6a**

By the general procedure: step 1, **4** (0.104 g, 0.444 mmol) was dissolved in dry DCM/DMF (22.2 mL/22.2 mL; 10 mmol/L). HBTU (0.404 g, 1.066 mmol), **3a** (0.500 g, 0.977 mmol), and triethylamine (0.25 mL, 1.8 mmol) were subsequently added; step 2, TFA (5 mL) and the product of step 1; a waxy light yellow solid was afforded in 53% yield (0.264 g). Data for **5a**: ^{1}H NMR (300 MHz, $CDCl_3$) δ: 7.02 (d, 2H, J = 8.6 Hz), 4.46 (m, 2H), 4.24 (m, 4H), 4.12 (m, 4H), 3.25 (s, 4H), 2.31 (t, 8 H, J = 7.8 Hz), 1.59 (m, 8H), 1.25 (s, 80H), 0.87 (t, 12H, J = 6.9 Hz). ^{13}C NMR (75 MHz, $CDCl_3$) δ: 174.0, 170.8, 62.9, 52.8, 48.0, 34.3, 32.1, 29.9, 29.9, 29.7, 29.6, 29.5, 29.4, 25.1, 22.9, 14.3. MS ((+) ESI): calcd for $C_{66}H_{126}N_3O_{10}^+$, 1120.94 amu,;found, 1121.00 amu. Continuing the general procedure: step 3, Boc-glycine (0.033 g, 0.19 mmol) in dried DCM/DMF (9.0 mL/9.0 mL; 10 mmol/L), HOBt (0.029 g, 0.21 mmol), HBTU (0.080 g, 0.21 mmol), **5a** (0.20 g, 0.179 mmol), and triethylamine (0.075 mL, 0.53 mmol); step 4, TFA (5 mL) and the Boc-protected product gave a light brown solid that was used without additional purification.

5b *and* **6b**

By the general procedure: step 1, **4** (0.093 g, 0.40 mmol) was dissolved in dry DCM/DMF (20.0 mL/20.0 mL; 10 mmol/). HBTU (0.364 g, 0.960 mmol), **3b** (0.500 g, 0.880 mmol), and triethylamine (0.22 mL, 1.6 mmol) were subsequently added; step 2, TFA (5 mL) and the Boc-protected product of step 1; a light brown waxy solid was afforded in 55% yield (0.272 g). Data for **5b** ^{1}H NMR (300 MHz, $CDCl_3$) δ: 7.03 (d, 2H, J = 8.7 Hz), 4.47 (m, 2H), 4.26 (m, 4H), 4.14 (m, 4H), 3.27 (s, 4H), 2.33 (t, 8H, J = 7.3 Hz), 1.60 (m, 8H), 1.27 (s, 96H), 0.89 (t, 12H, J = 6.8). ^{13}C NMR (75 MHz, $CDCl_3$) δ: 174.0, 170.8, 62.8, 52.7, 48.0, 34.31, 32.1, 29.9, 29.7, 29.6, 29.5, 29.4, 25.1, 22.9, 14.3. MS ((+) ESI): calcd for $C_{74}H_{142}N_3O_{10}^+$, 1233.07 amu; found, 1233.00. Continuing the general procedure: step 3, Boc-glycine (0.030 g, 0.17 mmol) in dried DCM/DMF (8.1 mL/8.1 mL; 10 mmol/L), HOBt (0.026 g, 0.20 mmol), HBTU (0.074 g, 0.20 mmol), **5b** (0.201, 0.162 mmol), and triethylamine (0.068 mL, 0.49 mmol); step 4, TFA (5 mL) and the Boc-protected product of step 3 gave a light brown oil that was used without further purification. MS ((+) ESI): calcd for $C_{76}H_{145}N_4O_{11}^+$, 1290.09 amu; found, 1290.00 amu.

5c *and* **6c**

By the general procedure: step 1, **4** (1 equiv.) was dissolved in dry DCM/DMF (1:1; 10 mmol/L). HBTU (0.363 g, 0.960 mmol), **3c** (0.500 g, 0.880 mmol), and triethylamine (0.22 mL, 1.6 mmol) were subsequently added; step 2, TFA (5 mL) and the Boc-protected product of step 1; a colorless oil was afforded in 60% yield (0.296 g). Data for **5c** ^{1}H NMR (300 MHz, $CDCl_3$) δ: 7.07 (d, 2H, J = 8.6 Hz), 4.46 (m, 2H), 4.25 (m, 4H), 4.11 (m, 4H), 3.23 (s, 4H), 2.34 (m, 4H), 1.56, 1.45 (m, 16H), 1.24 (s, 80H), 0.86 (t, 24H, J = 7.4 Hz). ^{13}C NMR (75 MHz, $CDCl_3$) δ: 176.4, 170.4, 62.3, 52.6, 48.0, 45.6, 34.6, 34.4, 32.9, 32.7, 32.5, 32.3, 32.2, 31.8, 31.6, 31.5, 29.6, 29.5, 29.4, 29.2, 29.2, 29.0, 27.4, 27.4, 25.2, 22.6, 22.6, 20.6, 14.0, 14.0, 11.3. MS ((+) ESI): calcd for $C_{74}H_{142}N_3O_{10}^+$, 1233.07 amu; found, 1232.87 amu. Continuing the general procedure: Boc-glycine (0.030 g, 0.17 mmol) in dried DCM (1.62 mL), HOBt (0.026 g, 0.20 mmol), HBTU (0.074 g, 0.20 mmol), **5c** (0.200 g, 0.162 mmol), and triethylamine (0.068 mL, 0.49 mmol); step 4, TFA (5 mL) and the Boc-protected product of step 3 gave a light brown oil that was used without further purification. MS ((+) ESI): calcd for $C_{76}H_{145}N_4O_{11}^+$, 1290.09 amu; found, 1289.93 amu.

5d *and* **6d**

By the general procedure: step 1, **4** (0.088 g, 0.36 mmol) was dissolved in dried DCM/DMF (18.2 mL/18.2 mL; 10 mmol/L). HBTU (0.329 g, 0.867 mmol), **5d** (0.500 g, 0.801 mmol), and triethylamine (0.20 mL, 1.5 mmol) were subsequently added; step 2, TFA (5 mL) and the Boc-protected product of step 1; as a white waxy solid in a 51% yield (0.248 g). Data for **5d**: ^{1}H NMR (300 MHz, $CDCl_3$) δ: 7.07 (d, 2H, J = 8.6 Hz), 4.46 (m, 2H), 4.25 (m, 4H), 4.13 (m, 4H), 3.26 (s, 4H), 2.32 (t, 8H, J = 7.8 Hz), 1.60 (m, 8H) 1.25 (s, 112H), 0.87 (t, 12H, J = 6.8 Hz). ^{13}C NMR (75 MHz, $CDCl_3$) δ: 174.0, 170.8, 62.9, 52.8, 48.1, 34.3, 32.1, 29.9, 29.7, 29.6, 29.5, 29.4, 25.1, 22.9, 14.3. MS ((+) ESI): calcd for $C_{82}H_{158}N_3O_{10}^+$, 1345.19 amu; found, 1345.07 amu. Continuing the general procedure: step 3, Boc glycine (0.013 g, 0.074 mmol) in dried DCM/DMF (3.7 mL/3.7 mL; 10 mmol/L), HOBt (0.012 g, 0.085 mmol), HBTU (0.032 g, 0.085 mmol), **5d** (0.0950 g, 0.0706 mmol), and triethylamine (0.030 mL, 0.21 mmol); step 4, TFA (5 mL) and the Boc-protected product of step 3 gave a light brown oil that was used without further purification.

Asymmetric disulfide synthesis — preparation of 8

In a round-bottom flask, 6-mercaptopurine monohydrate (0.500 g, 2.94 mmol) and 11-thioundecanoic acid (0.641 g, 2.94 mmol) were dissolved in DMSO (9.0 mL; 0.33 mol/L). While the reaction was stirred, solid DDQ (0.669 g, 2.94 mmol) was slowly added over 10 min, and then, the mixture was left at room temperature for 1 h. The reaction was monitored by TLC (silica gel, MeOH/DCM as eluent, visualized by iodine). Following completion, the product was precipitated by adding 20 mL of water to the reaction solution. The resulting mixture was left for 6 h before being vacuum filtered and a red solid was isolated. The crude product was redissolved in hot methanol, cooled in an ice water bath, and then, vacuum filtered. A white powder was afforded in a 60% yield (0.622 g). ^{1}H NMR (300 MHz, DMSO-d^6) δ: 8.84 (s, 1H), 8.57 (s, 1H), 2.96 (t, 2H, J = 7.0 Hz), 2.21 (t, 2H, J = 7.3 Hz), 1.67 (quintet, 2H, J = 7.5 Hz), 1.50, 1.40 (m, 4H), 1.25 (s, 10H). ^{13}C NMR (75 MHz, DMSO-d^6) δ: 174.4, 151.7, 39.5, 38.1, 33.6, 28.8, 28.7, 28.5, 28.1, 27.6, 24.5. (MS ((+) ESI): calcd for $C_{16}H_{25}N_4O_2S_2^+$, 369.14 amu; found, 369.13 amu.

Similarly, in a round-bottom flask, 6-thioguanine (0.500 g, 2.99 mmol) and 11-thioundecanoic acid (0.652 g, 2.99 mmol) were dissolved in DMSO (0.15 mol/L). While the reaction was stirred, solid DDQ (0.679 g, 2.99 mmol) was slowly added over 10 min, and then, the mixture was left at room temperature for 1 h. The reaction was monitored by TLC (silica gel, MeOH/DCM as eluent, visualized by iodine). Following completion, the product was precipitated by adding water to the reaction solution. The resulting mixture was left for 6 h before being vacuum filtered and a red solid was isolated. The crude product was redissolved in hot acetone, cooled in an ice water bath, and then, vacuum filtered. A yellowish powder was afforded in 64% yield (0.707 g). ^{1}H NMR (300 MHz, DMSO-d^6) δ: 7.98 (s, 1H), 6.45 (s, 2H), 2.90 (t, 2H, J = 7.1 Hz), 2.17 (t, 2H, J = 8.4 Hz), 1.62 (quintet, 2H, J = 7.0), 1.46, 1.35 (m, 4H), 1.21 (s, 10H). ^{13}C NMR (75 MHz, $CDCl_3$) δ: 174.5, 159.9 156.9, 140.1, 39.5, 38.10, 33.6, 28.8, 28.7, 28.5, 28.01, 27.7, 24.5. MS ((+) ESI): calcd for $C_{16}H_{26}N_5O_2S_2^+$, 384.15 amu; found, 384.27 amu.

General procedure for LDC monomer synthesis

In a round-bottom flask, **8** (1.1 equiv.) was dissolved in dried DCM/DMF (1:1; 10 mmol/L). To this, HBTU (1.2 equiv.), **3a–3d** (1.0 equiv.), and triethylamine (2.0 equiv.) were then added, and the resulting solution was left stirring at room temperature for 20 h. When the reaction was complete, visualized by ^{1}H NMR, the reaction solution was diluted with EtOAc and washed once with 1 mol/L HCl and three times with H_2O. The organic layer was dried over anhydrous sodium sulfate and then gravity filtered. DCM and EtOAc were removed by rotary evaporation. The crude product was purified by flash column chromatography on silica, using EtOAc/hexanes as the eluent.

MP-C14

By the general procedure: **6-MP** (0.113 g, 0.308 mmol) was dissolved in dried DCM/DMF (14.6 mL/14.6 mL; 10 mmol/L). HBTU (0.133 g, 0.352 mmol, 1.20 equiv.), **3a** (0.150 g, 0.293 mmol), and triethylamine (0.082 mL, 0.59 mmol) were subsequently added; a

light yellow solid was afforded in a 28% yield (0.072 g). ^{1}H NMR (300 MHz, $CDCl_3$) δ: 11.75 (s, 1H), 8.90 (s, 1H), 8.22 (s, 1H), 6.02 (d, 1H, J = 8.3 Hz) 4.52 (m, 1H), 4.30 (m, 2H), 4.11 (m, 2H), 2.91(t, 2H, J = 7.0 Hz), 2.32 (t, 4H, J = 7.9 Hz), 2.02 (t, 2H, J = 7.9 Hz), 1.66 (m, 6H), 1.26, 1.12 (m, 54H), 0.88 (t, 6H, J = 7.0). MS ((+) ESI): calcd for $C_{47}H_{84}N_5O_5S_2^+$, 862.59 amu; found, 862.53 amu.

MP-C16

By the general procedure: **6-MP** (0.0648 g, 0.176 mmol) was dissolved in dried DCM/DMF (9.0 mL/9.0 mL; 10 mmol/L). HBTU (0.112 g, 0.211 mmol), **3b** (0.0648 g, 0.176 mmol), and triethylamine (0.076 mL, 0.53 mmol) were subsequently added; a white solid was afforded in a 63% yield (0.102 g). ^{1}H NMR (300 MHz, $CDCl_3$) δ: 12.88 (s, 1H), 8.91 (s, 1H), 8.29 (s, 1H), 6.05 (d, 1H, J = 8.2 Hz), 4.50 (m, 1H), 4.26 (m, 2H), 4.09 (m, 2H), 2.91 (t, 2H, 7.1 Hz), 2.30 (t, 4H, J = 7.6 Hz), 2.20 (t, 2H, J = 7.1 Hz), 1.65 (m, 6H), 1.24, 1.17 (m, 62H), 0.87 (t, 6H, J = 6.9 Hz). ^{13}C NMR (75 MHz, $CDCl_3$) δ: 174.1, 173.8, 160.5, 152.6, 149.9, 142.0, 131.4, 62.9, 48.0, 39.3, 36.9, 34.3, 32.1, 29.9, 29.9, 29.8, 29.7, 29.6, 29.5, 29.4, 29.1, 28.7, 28.3, 25.9, 25.1, 22.9, 14.3. MS ((+) ESI): calcd for $C_{51}H_{92}N_5O_5S_2^+$, 918.65 amu; found, 918.60 amu.

MP-bC16

By the general procedure: **6-MP** (0.136 g, 0.370 mmol) was dissolved in dried DCM/DMF (17.5 mL/17.5 mL; 10 mmol/L). HBTU (0.160 g, 0.422 mmol), **3c** (0.200 g, 0.352 mmol), and triethylamine (0.126 mL, 0.704 mmol) were subsequently added; a light yellow oil was afforded in a 42% yield (0.137 g). ^{1}H NMR (300 MHz, $CDCl_3$) δ: 12.8 (s, 1H), 8.90 (s, 1H), 8.29 (s, 1H), 5.97 (d, 1H, J = 8.8 Hz), 4.48 (m, 1H), 4.26 (m, 2H), 4.09 (m, 2H), 2.90 (t, 2H, J = 7.3 Hz), 2.32 (m, 2H), 2.2 (m, 2H), 1.68, 1.55, 1.42 (m, 14H), 1.22, 1.16 (m, 50H), 0.85 (t, 12H, J = 6.9 Hz). ^{13}C NMR (75 MHz, $CDCl_3$) δ: 176.5, 173.3, 152.2, 142.0, 62.4, 48.0, 45.6, 39.1, 36.7, 32.3, 32.0, 31.8, 31.6, 29.7, 29.5, 29.4, 29.2, 29.2, 28.9, 28.5, 28.2, 27.4, 27.4, 25.6, 22.6, 22.6, 14.0, 14.0. MS ((+) ESI): calcd for $C_{51}H_{92}N_5O_5S_2^+$, 918.65 amu; found, 918.53 amu.

MP-C18

By the general procedure: **6-MP** (0.062 g, 0.168 mmol) was dissolved in dried DCM/DMF (8.0 mL/8.0 mL; 10 mmol/L). HBTU (0.073 g, 0.19 mmol), **3d** (0.100 g, 0.160 mmol), and triethylamine (0.045 mL, 0.32 mmol) were subsequently added; a white solid was afforded in a 32% yield (0.050 g). ^{1}H NMR (300 MHz, $CDCl_3$) δ: 8.91 (s, 1H), 8.27 (s, 1H), 6.01 (d, 1H, J = 8.3 Hz), 4.50 (m, 1H), 4.26 (m, 2H), 4.09 (m, 2H), 2.90 (t, 2H, J = 7.2 Hz), 2.30 (t, 4H, J = 7.8 Hz), 2.20 (t, 2H, J = 7.8 Hz), 1.68, 1.59 (m, 6H), 1.24, 1.15 (m, 70H), 0.87 (t, 6H, J = 6.9 Hz). ^{13}C NMR (75 MHz, $CDCl_3$) δ: 173.8, 173.5, 152.3, 62.7, 47.7, 39.1, 36.7, 34.1, 31.9, 29.7, 29.6, 29.5, 29.3, 29.2, 29.1, 29.1, 29.0, 28.9, 28.8, 28.4, 28.0, 25.6, 24.9, 22.7, 14.1. MS ((+) ESI): calcd for $C_{55}H_{100}N_5O_5S_2^+$, 974.72 amu; found, 974.67 amu.

TG-C14

By the general procedure: **6-TG** (0.118 g, 0.308 mmol) was dissolved in dried DCM/DMF (14.6 mL/14.6 mL; 10 mmol/L). HBTU (0.133 g, 0.352 mmol), **3a** (0.150 g, 0.293 mmol), and triethylamine (0.082 mL, 0.586 mmol) were subsequently added; a light yellow solid was afforded in 18% yield (0.047 g). ^{1}H NMR (300 MHz, $CDCl_3$) δ: 7.92 (s, 1H), 6.10 (d, 1H, J = 8.10 Hz), 5.31 (s, 2H), 4.52 (m, 1H), 4.29 (m, 2H), 4.12 (m, 2H), 2.88 (t, 2H, J = 7.3 Hz), 2.32 (t, 4H, J = 7.3 Hz), 2.18 (t, 2H, J = 7.3 Hz), 1.68, 1.59 (m, 6H), 1.25, 1.18 (m, 54H), 0.88 (t, 6H, J = 6.9 Hz). ^{13}C NMR (75 MHz, $CDCl_3$) δ: 174.1, 173.7, 159.7, 139.6, 63.0, 48.0, 39.4, 36.9, 34.3, 32.1, 29.9, 29.9, 29.8, 29.7, 29.6, 29.5, 29.4, 29.4, 29.3, 29.1, 28.7, 28.3, 25.8, 14.3. MS ((+) ESI): calcd for $C_{47}H_{85}N_6O_5S_2^+$, 877.60 amu; found, 877.67 amu.

TG-C16

By the general procedure: **6-TG** (0.068 g, 0.18 mmol) was dissolved in dried DCM/DMF (8.8 mL/8.8 mL; 10 mmol/L). HBTU (0.112 g, 0.211 mmol), **3b** (0.120 g, 0.18 mmol), and triethylamine (0.076 mL, 0.53 mmol) were subsequently added; a light yellow solid was afforded in a 49% yield (0.081 g). ^{1}H NMR (300 MHz, $CDCl_3$) δ: 11.23 (s, 1H), 7.87 (s, 1H), 6.08 (d, 1H, J = 8.4 Hz), 5.24 (s, 2H), 4.51 (m, 1H), 4.29 (m, 2H), 4.11 (m, 2H), 2.87 (t, 2H, J = 7.0 Hz), 2.31 (t, 2H, J = 7.5 Hz), 2.17 (t, 2H, J = 7.6 Hz), 1.68, 1.60 (m, 6H), 1.24, 1.17 (m, 62H), 0.87 (t, 6H, J = 7.0 Hz). ^{13}C NMR (75 MHz, $CDCl_3$): 173.9, 173.5, 159.4, 62.8, 47.7, 39.2, 36.6, 34.1, 31.9, 29.7, 29.6, 29.4, 29.3, 29.2, 29.1, 29.0, 29.0, 28.8, 28.4, 28.1, 25.6, 24.9, 22.7, 14.1. MS ((+) ESI): calcd for $C_{51}H_{93}N_6O_5S_2^+$, 933.66 amu; found, 933.73 amu.

TG-bC16

By the general procedure: **6-TG** (0.071 g, 0.19 mmol) was dissolved in dried DCM/DMF (8.8 mL/8.8 mL; 10 mmol/L). HBTU (0.080 g, 0.21), **3c** (0.100 g, 0.176 mmol), and triethylamine (0.049 mL, 0.35 mmol) were subsequently added; a light yellow liquid was afforded in a 37% yield (0.061 g). ^{1}H NMR (300 MHz, $CDCl_3$) δ: 7.88 (s, 1H), 6.05 (d, 1H, J = 8.2 Hz), 5.20 (s, 2H), 4.50 (m, 1H), 4.30 (m, 2H), 4.12 (m, 2H), 2.87 (t, 2H, J = 7.1 Hz), 2.35 (m, 2H), 2.15 (t, 2H, J = 7.4 Hz), 1.68, 1.57, 1.45 (m, 14H), 1.24, 1.16 (m, 50H) 0.86 (t, 12H, J = 6.5 Hz). ^{13}C NMR (75 MHz, $CDCl_3$) δ: 176.7, 173.3, 159.4, 62.5, 48.0, 45.7, 39.1, 36.6, 32.3, 31.8, 31.6, 29.7, 29.6, 29.4, 29.3, 29.2, 29.1,29.0, 29.0, 28.8, 28.4, 28.0, 27.4, 27.4, 25.5, 22.6, 22.6, 14.1, 14.00. MS ((+) ESI): calcd for $C_{51}H_{93}N_6O_5S_2^+$, 933.66 amu; found, 933.60 amu.

General procedure for PEG-lipids

An equimolar mixture of **7** and the amino lipid was made to a concentration of 0.12 mol/L in pyridine in a vial. The vial was then sealed, and the solution was heated to 55 °C and stirred for 48 h. Following completion, as monitored by TLC (silica gel, MeOH/DCM as eluent, visualised by iodine), the pyridine was removed on a rotary evaporator and the resulting mixture was purified by flash column chromatography on silica gel, using MeOH/DCM as the eluent. The amounts used and the characteristic ESI–MS are given in full in the Supplementary material.

Preparation of LNPs

Stock solutions of lipids were made up in ethanol with a lipid concentration of 10 mmol/L. In an Eppendorf tube, the lipid mixture of PEG-lipid (5.00 mol %), DMPC (5.00 mol %), and LDC (90.00 mol %) was made up to a total volume of 0.25 mL with additional ethanol. The mixture was then heated to 43 °C for 5 min in the oven.

Prior to using, the NanoAssemblr™ cartridge was washed with PBS buffer in a 3 mL syringe (left port) and ethanol in a 3 mL syringe (right port) with a 12 mL/min flow rate and a 1:1 (aqueous: ethanol) flow ratio. A total of 4 mL of wash was collected and discarded. The NanoAssemblr™ microfluidic mixer was then used to make the LNPs. A 3 mL syringe (left port) was loaded with 2 mL PBS buffer and another 3 mL syringe (right port) was loaded with the 0.25 mL lipid mixture. The flow rate was set to 4 mL/min, the flow ratio was set to 3:1 (aqueous:EtOH), and the total volume collected was 1 mL, with the initial 300 uL at the beginning and 50 uL at the end being discarded. An aliquot (0.50 mL) of the collected formulation was then diluted to 0.40 mmol/L (thiopurine) with PBS buffer, transferred to a 3 mL Slide-A-Lyzer® Dialysis Cassette G2 (10 000 molecular weight cutoff), and dialyzed against PBS buffer for 5 h. The PBS buffer was refreshed after 3 h, and the removal of ethanol from the formulation was monitored using potassium dichromate. Diameters of the SNPs were determined by dynamic light scattering (DLS) experiments (Brookhaven Instrument, ZetaPALS particle sizing software). The SNPs were then stored at 4 °C.

Stability assay methods

The stability of the formulated LNPs was assessed under six conditions: LNPs were stored at three different temperatures, i.e., 4 °C, ambient, and 37 °C, and incubated in two different media, namely PBS buffer and PBS buffer with 10% bovine growth serum (BGS; by volume). To a polystyrene cuvette, 200 uL of LNPs solution

Scheme 2. Synthesis of serinol-derived branched and dendritic lipids. Boc, tert-butoxycarbonyl; DCM, dichloromethane; DMF, N,N,-dimethylformamide; Gly, glycine; HBTU, N,N,N′N′-tetramethyl-O(1H-benzotriazol-1yl) uronium hexfluorophosphate; HOBT, hydroxybenzotriazole; NHS, N-hydroxysuccimidyl; pyr, pyridine; TFA, trifluoroacetic acid.

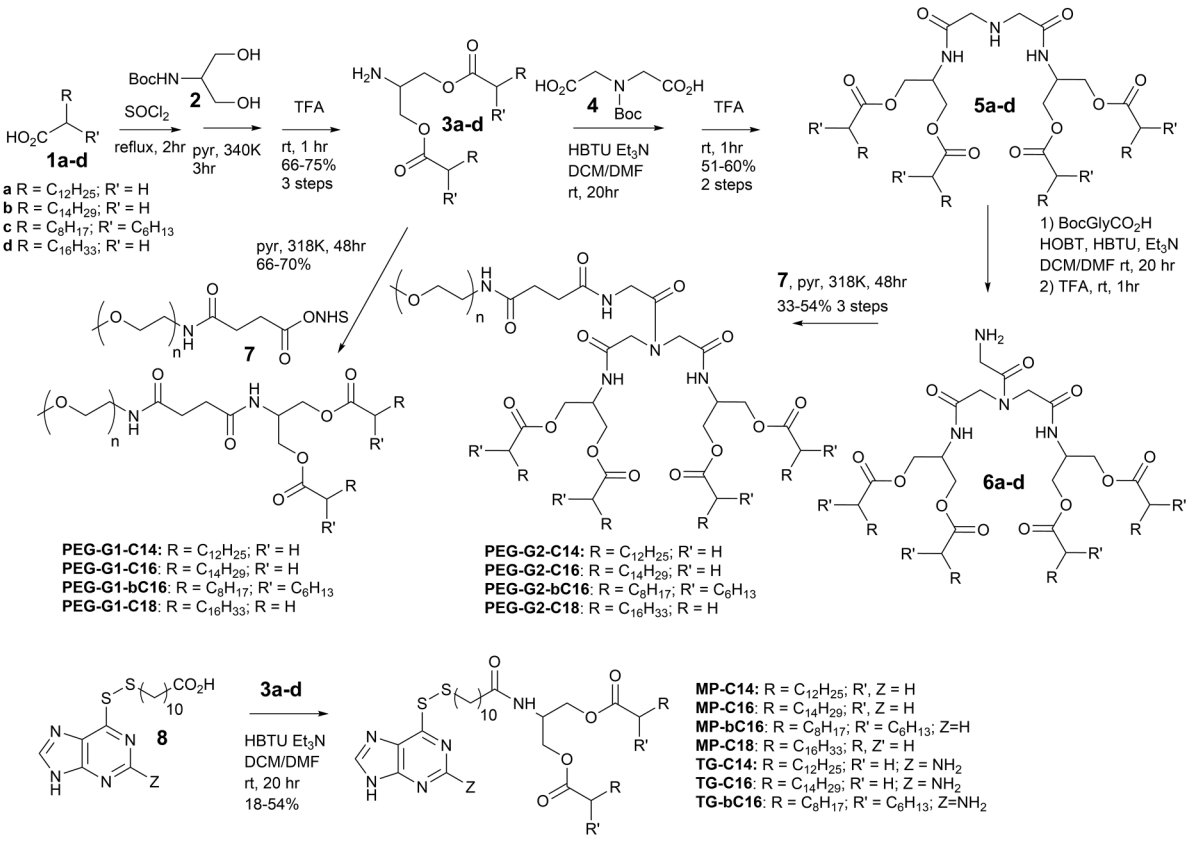

and 2.30 mL of PBS buffer, or 2.05 mL of PBS buffer and 0.25 mL of serum, were added and the diameters measured in a DLS experiment. Cuvettes were then sealed and incubated under the indicated conditions. Diameter measurements were taken regularly. Full data are given in the Supplementary material.

Bioassay methods

MCF7 cells were seeded on 24 well plates at 5.0×10^4 cells/well, 18 h later were treated with the indicated compounds in growth medium (Dulbecco's Modified Eagle's Medium (DMEM) supplemented with 10% BGS). DMSO was used at a concentration of 400 μmol/L in growth medium as a control for 6-thioguanine (**6-TG**) and 6-mecaptopurine (**6-MP**), and Na_3PO_4 buffer (pH 7, $[Na_3PO_4] = 10$ mmol/L [NaCl] = 0.1 M) was used at a concentration of 40 μmol/L in growth medium as a control for **6TG-C16**, **6TG-bC16**, **6MP-C16**, and **6MP-bC16**. After 72 h of treatment, cells were washed with phosphate-buffered saline (PBS), fixed for 10 mins with 4% paraformaldehyde in PBS, stained for 30 mins with 0.1% crystal violet in H_2O, washed twice with H_2O, and let dry. Then, 10% acetic acid was added to wells and incubated on a shaker for 10 mins. Absorbance was measured at 590 nm using a PerkinElmer Victor³V 1420 multilabel plate counter. The absorbance from stained wells without cells was subtracted from experimental values to eliminate background absorbance from crystal violet adhering to the plate. The percent viability was calculated as follows: (absorbance compounds/absorbance control buffer) × 100. A subset of the data is given in the figures; the full data are given in the Supplementary material.

A one-way ANOVA was performed for the experiments on MCF-7 cells: **6-TG**, $F_{[7,16]} = 243.8$ and $P < 0.001$; **6-MP**, $F_{[7,16]} = 18.77$ and $P < 0.001$; **6TG-C16**, $F_{[5,12]} = 23.58$ and $P < 0.001$; **6TG-bC16**, $F_{[5,12]} = 24.97$ and $P < 0.001$; **6MP-C16**, $F_{[5,12]} = 18.21$ and $P < 0.001$; **6MP-C16**, $F_{[5,12]} = 18.16$ and $P < 0.001$, followed by Tukey's multiple-comparison posthoc test to determine whether there were significant differences between groups.

A one-way ANOVA was also performed for the experiments on HeLa cells: **6-TG**, $F_{[7,16]} = 24.69$, $P < 0.001$; **6-MP**, $F_{[7,16]} = 13.37$ and $P < 0.001$; **6TG-C16**, $F_{[6,14]} = 26.51$ and $P < 0.001$; **6TG-bC16**, $F_{[6,14]} = 2.06$ and $P > 0.05$; **6MP-C16**, $F_{[6,17]} = 2.24$ and $P > 0.05$; **6MP-bC16**, $F_{[6,14]} = 0.57$ and $P > 0.05$, followed by Tukey's multiple-comparison posthoc test to determine whether there were significant differences between groups.

Results and discussion

Synthesis

The serinol-based lipids **3a–3d** were readily accessed (Scheme 2) in good yields over three steps, requiring only extractive workup to isolate the pure lipid anchors. The diaseterotopic serinol-derived methylene protons appear as complex but symmetric multiplets in the ¹H NMR spectra (see Supplementary material).

Dendritic analogues **5a–5d** were synthesized in moderate yields over two steps utilizing an iminodiacetic acid backbone and **3a–3d**. Once again, extractive workups were all that were necessary to access the pure lipids. The methylene protons present in the serinol fragment were observed here as two distinct multiplets in the ¹H NMR (see Supplementary material).

Conjugates of **3a–3d** with thiopurine drugs requires a suitable disulfide that we elected to incorporate via a C_{11} spacer. Oxidation with DDQ of an equimolar mixture of 11-thioundecanoic acid and either 6-mercaptopurine or 6-thioguanine provides the asymmetric disulfides **8** with excellent selectivity following simple precipitation and recrystallization. Only the asymmetric disulfide **8** was observed by both ¹H NMR and ESI–MS. This type of heteroselec-

Fig. 1. Electrospray mass spectrum of **PEG-G2-C14 (**0.1% TFA and 0.1% NaCl in methanol). The compound shows four distinct ion series for PEG-oligomers bearing $4Na^+$ (yellow inverted triangle), $3Na^+$ (red squares), $2Na^+$ and H^+ (grey squares), and $2Na^+$ (blue circles). A total of 64 of the 71 isotopic ion clusters are assigned to a specific value of the number of ethyleneoxy units in the PEG (*N*). The inset shows the sum of ion intensities for a given value of *N* (where observed and assigned). The curve is a Gaussian fit to the data (center, 43.1 ± 0.13; width, 11 ± 1.7; r^2 = 0.969). [Colour online.]

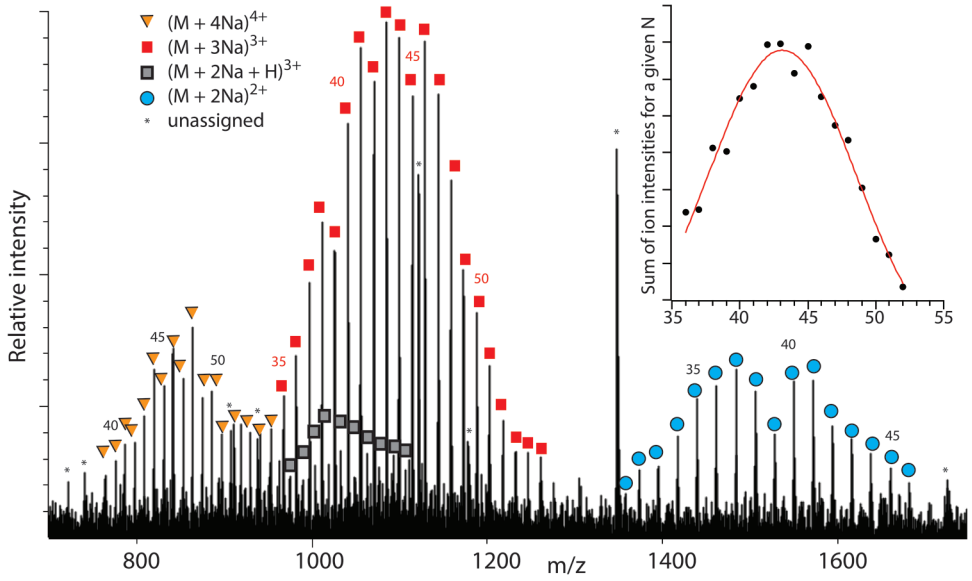

tively has been demonstrated for aromatic thiols forming disulfides with alkyl thiols.[40] Amide coupling of **8** with lipid anchors **3a–3d** afforded the seven LDC monomers in poor to moderate yields — providing sufficient material to explore the composition space for the LDC nanoparticle formulations.

Linkage of the PEG to the lipid anchors required some optimization. Initially, we expected to use an isocyanate-terminated PEG2000 derivative; two different commercial samples failed to give any evidence of the expected carbamate products (NMR, IR, ESI–MS). N-hydrosuccinimide PEG2000 **7** is reported to react readily at hindered sites in proteins at ambient temperature;[41] **7** did react with **3a–3d** in pyridine at a slow rate; moderate heating over 48 h in pyridine was required to produce the first generation PEG-lipids (**PEG-G1-C#**) in yields of 66%–70% following chromatographic purification. The NHS–PEG derivative **7** did not react with the secondary amine of **5a–5d** at an appreciable rate, so we elected to install a glycine spacer to produce a primary amine (**6a–6d**) for coupling. The final step of the dendritic PEG-lipid synthesis proceeded from coupling of **7** with the unpurified **6a–6d** under the same conditions as used previously with **3a–3d** to give **PEG-G2-C#** in 33%–54% chromatographed yield for the three steps from **5a–5d**.

Structural confirmation of the PEG lipids based on ^{1}H NMR proved to be complex. Amide formation for **3a–3d** was confirmed by the downfield shift of the methine proton on the serinol backbone from 3.28 ppm (amine) to 4.41 ppm (amide); a similar shift of the glycine-derived methylene signals in **PEG-G2-C#** samples similarly confirms amide coupling (see Supplementary material). Furthermore, due to lack of free bond rotation at the amide, the diastereomeric methylene protons on the serinol backbone experience a greater difference in chemical environment and, correspondingly, better resolved symmetrical multiplets in the amides relative to the starting amines. However, the commercial sample of **7** was contaminated to the extent of about 40 mol% with a bis-methoxy terminated oligomer MeO–PEG–OMe (see Supplementary Fig. S3). This impurity was not (fully) removed from the final samples by chromatography, and the integrations of the methoxy signals relative to the serinol-derived signals all show excess intensity in the methoxy singlet. The estimated purities based in integration range from 60 to 85 mol% for the **PEG-G*n*-C#** samples. This level of impurity can be tolerated in the proof-of-principle experiments described below; more detailed analyses will require starting materials with higher purity.

ESI–MS was used to characterize the PEG-lipids as the distribution of PEG oligomers. All PEG-lipids gave ESI spectra of ions bearing multiple cations grouped in clusters corresponding to different oligomers in the PEG chain (Fig. 1). No ions associated with the starting amines were observed. Nor were any ions associated with the known impurity MeO–PEG–OMe, presumably due to the high surfactant character of the PEG-lipids that would suppress ionization of weaker surfactants. The observed ions were assigned based on isotopic mass predictions to a given value of the number of ethyleneoxy units in the oligomer (*N*). The intensities for all observed ions of a given *N* were summed, and a Gaussian distribution was fit to determine the average *N* and distribution width of the sample. The starting NHS ester **7** gave a value of *N* = 43.5 ± 0.2 and a width of 14 ± 1.5; with the exception of **PEG-G2-bC16**, the isolated products gave *N* = 43.3 ± 0.3 and a width of 14 ± 5.3. This suggests that for the majority of samples there has been little fractionation during synthesis and handling and that the original distribution is relatively unaltered. The **PEG-G2-bC16** sample has much broader distributions of ions within each oligomer series observed, and the summed data do not fit well to a Gaussian distribution (r^2 < 0.7). The identity of the compound is not in doubt, but the spectra suggest that some fractionation has occurred or that the ionization of this compound differs from the rest of the series or both. Spectra similarly analyzed are given for all products in the Supplementary material.

LNP formulation and particle size stability

Recent advances in microfluidic mixing technologies allow the rapid, reproducible, and scalable production of LNPs.[12,42–45] The Precision Nanosystems microfluidic mixer (NanoAssemblr™) is based on a staggered herringbone design,[43] which leads to rapid mixing via chaotic advection and efficiently gives reproducible LNP formulations.[12,42,44] The mixer takes lipidic components in a water-miscible organic solvent such as ethanol and rapidly dilutes them into aqueous buffer to produce LNPs by hydrophobic

Fig. 2. Particle size during storage in PBS at 37 °C for LNP formulations containing 90 mol% **MP-C#** or **TG-C#,** 5 mol% DMPC, and 5 mol% PEG-DSPE. [Colour online.]

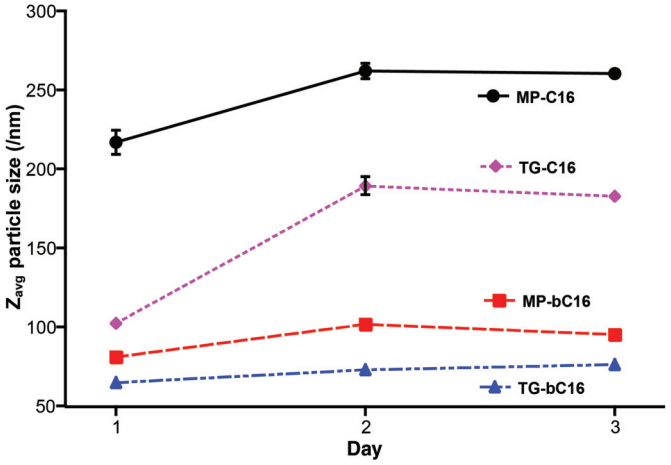

Fig. 3. Cell viability as a function of thiopurine dose level as assessed by a Crystal Violet assay. Top panel: for MCF-7 cells; bottom panel: for HeLa cells. **TG** (6-thioguanine) and **MP** (6-mercaptopurine) were added to the media at the indicated concentrations. The LNP formulations (90 mol% **MP-C#** or **TG-C#**, 5 mol% DMPC, and 5 mol% PEG-DSPE) were diluted to give the indicated total thiopurine concentration. Significant differences from buffer are as follows: **, $P < 0.01$; ***, $P < 0.001$. Error bars represent standard deviation. [Colour online.]

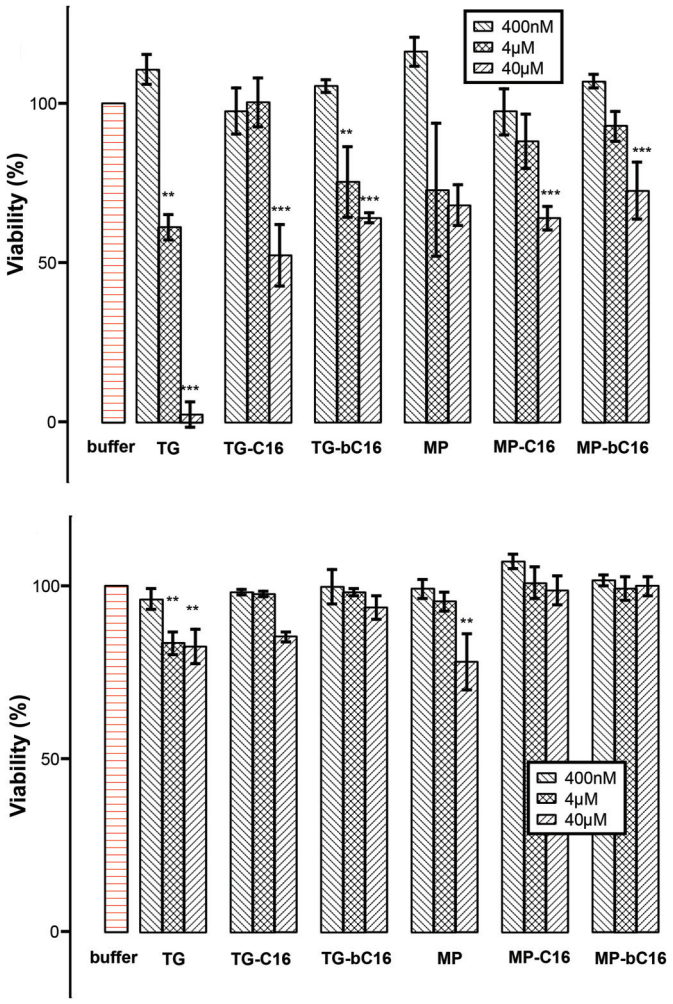

association of the components. Organic solvents and small molecules are readily removed by dialysis. Given the unusual structures of the branched and dendritic lipids prepared, we opted to use a standardized procedure as opposed to individual operating conditions and formulations requiring optimization. The reliability of LNP formation was assessed by particle size and polydispersity index (PDI), as determined by dynamic light scattering.

Neutral hydrophobic compounds dispersed in water rarely form stable self-assemblies on their own and usually crystallize or precipitate; initial attempts to form **MP-C#** and **TG-C#** monomers directly into LNPs confirmed this. Incorporation of a surfactant into the LDC formulations was therefore necessary to improve the solubility of the LNPs. Several different compositions were investigated before arriving at 5 mol% 1,2-dimyristoyl-sn-glycero-3-phosphocholine (DMPC), 5 mol% 1,2-distearoyl-sn-glycero-3-phosphoethanolamine-N-(methoxy- (polyethylene glycol)-2000) (ammonium salt) (DSPE-PEG), and 90 mol% **MP-C#** or **TG-C#**. The drug loading for all of these formulations was 15 wt% calculated from the thiopurine drug mass over the total mass of the mixture.

Particle stability was evaluated by monitoring particle size and PDI over time in PBS or 10% serum in PBS at various temperatures (4 °C, ambient, 37 °C). An increase in particle size and (or) PDI was taken as an indication of particle aggregation as a result of particle instability.[46] **MP-C14**, **MP-C18**, and **TG-C14** showed significant size increase (45%–100% diameter increase) after 30 days at 4 °C in PBS buffer (Supplementary Tables S3–S9). The LNPs from **MP-C16**, **MP-bC16**, **TG-C16**, and **TG-bC16** maintain their apparent diameters (0%–20% diameter increase) and PDI values (–10% to 10% PDI change) for up to 60 days at 4 °C (see Supplementary material). At 37 °C in PBS, the isomeric pairs **MP-C16**/**MP-bC16**, and **TG-C16**/**TG-bC16** show significant differences in stability, with the branched chain isomers giving the apparently more stable LNPs (Fig. 2).

In the MCF-7 tumour cell line, LNPs containing **MP-C16**, **MP-bC16**, **TG-C16**, and **TG-bC16** show activity in the same concentration range as the free drug (Fig. 3, top panel; Supplementary Figs. S13–S18). Control experiments show the same LNPs are generally inactive in HeLa cells (Fig. 3, bottom panel; Supplementary Figs. S19–S24), which contain normal cytosolic concentration and distribution of thiol/glutathione.[47] However, HeLa cells in this assay are not particularly sensitive to the thiopurines as free drugs so small differences will be missed. Taking the two bioassays in conjunction, there is indirect evidence that the LNPs are taken up by the MCF-7 tumour cell-line prior to reduction and thereafter release the thiopurine in the cytosol. Although it is unclear if there is an isomer difference in these bioassays, we are encouraged by the apparent stability of the LNPs under the physiological conditions needed for cell proliferation.

Turning to assessment of the PEG-lipid compounds, these were formulated into LNPs similar to those for siRNA transfection experiments,[12] using a double-stranded DNA (dsDNA) octadecamer as the nucleic acid cargo. The **PEG-G1-C#** compounds (1.5 mol%) were formulated with the cationic lipid DOTMA (1,2-di-O-octadecenyl-3-trimethylammonium propane; 50 mol%), disteroylphosphatidyl choline (DSPC, 10 mol%), and cholesterol (38.5 mol%) at a N/P ratio of five with the dsDNA. The formulations were compared with the commercial DSPE-PEG bearing the same PEG oligomer length (Fig. 4; Supplementary Tables S10–S14).

Particle stability was assessed under various conditions; the results for 37 °C in PBS are given in Fig. 4A. Initial differences in the sizes of the LNPs indicate the formulation is not optimal for the complete set of PEG-lipids. The branched **PEG-G1-bC16** shows a markedly different time-dependent change under these conditions. A better cationic lipid for LNP formulation was available in a proprietary mixture,[12,48] as shown in Fig. 4B for **PEG-G2-C16**

Fig. 4. Particle size during storage for LNPs incubated at 37 °C in PBS for formulations containing 1.5 mol% of different PEG-lipids. (A) Composition, 50:10:38.5:1.5 of DOTMA:DSPC:Cholesterol:PEG-lipid. (B) Composition, 50:10:38.5:1.5 of ionisable lipid:DSPC: Cholesterol:PEG-lipid. Both experiments had a dsDNA loading of 5.1 wt%. Error bars are shown only when they exceed the symbol dimension. [Colour online.]

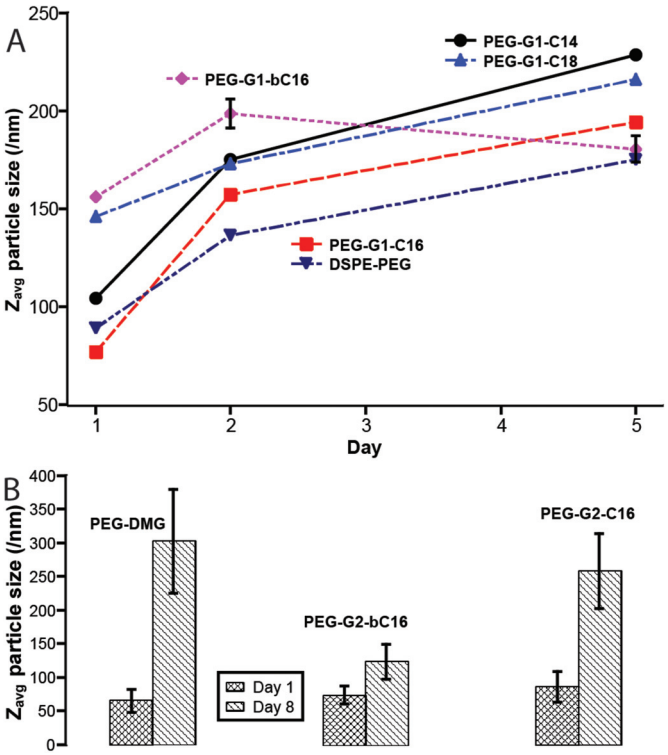

and **PEG-G2-bC16**; the neutral glycerol PEG ether DMG-PEG (1,2-Dimyristoyl-sn-glyceroxy-ω-methoxy poly-ethylene glycol; $n \sim 45$) was the control in these experiments (Fig. 4B; Supplementary Table S15). All three LNP formulations initially have 60–90 nm particle diameters, and are nearly monodisperse, but it is clear that the branched formulation containing **PEG-G2-bC16** is substantially more robust than even the commercial PEG-lipid under these conditions. Note that the lipid mixture used has been optimized for use with this commercially available PEG-lipid.

Conclusions

The synthesis of a new class of branched-chain and dendritic lipids derived from serinol was achieved. The yields are acceptable overall and produce materials in good quantities for formulations. As in other lipid amphiphile syntheses, chromatographic and handling losses can be significant, and many of the steps have been developed to avoid chromatography. The lipid amphiphiles give strong electrospray mass spectra, and in the case of the PEG-lipids prepared, the complex spectra could be analysed to establish the characteristics of the oligomeric PEG mixture. Not all PEG derivatives give this sort of diagnostic characterization tool. As an example, the impurity MeO–PEG–OMe in the commercial sample of **7** was clearly evident by ^{1}H NMR but absent in the ESI–MS spectra of mixtures containing it as a known impurity.

The lipids prepared have very unusual shapes compared with naturally occurring phospholipids. The lipid shape or packing parameter $S = V/a_0 l_c$ is derived from the volume of the lipid molecule (V), the projected area of the headgroup in the lipid interfacial plane (a_0), and the length of the hydrocarbon chains (l_c). Phospholipids based on diacylglycerols have $0.7 < S < 1$ predictive of their preferred formation into lamellar phases.[10] Using methods based on the additive molecular parameters we have used previously,[49,50] we estimate for the protonated forms of **3b** $S = 1.4$, of **3c** $S = 2.2$, of **5b** $S = 2.4$, and of **5c** $S = 3.6$. These values, lying well above $S = 1$, indicate a propensity to form inverted lipid phases; however, these very high values are so far outside the shape parameters associated with conventional amphiphiles that the details require considerable further experimental exploration. The compounds are also very lipophilic with calculated clogP values[49,50] of about 14 for **3bc**·HCl, about 28 for **5c**·HCl, and about 32 for **5b**·HCl. It is perhaps relevant to the potential applications of these unusually shaped lipids that the most extreme example — **PEG-G2-bC16** — is the compound that failed to give an acceptable fit to the ESI–MS ions observed, suggesting that the compound was a poorer surfactant than its isomer and congeners.

Formulation of the thiopurine lipid–drug conjugates into stable LNPs required only minor amounts of added surfactant and PEG-lipid, resulting in a drug loading of 15 wt%. The bioassays suggest the LNPs are taken into the MCF-7 cells where elevated levels of reductants in the cytosol liberate the thiopurines to produce the cytotoxic effect. Relative to HeLa cells, where the cytosol level of reductants is not elevated, the LDCs produced lower levels of toxicity than the free drug in the medium. Neither cell line showed any additional toxicity due to serinol diesters in these preliminary studies.

In storage tests evaluated by particle size change, there was a significant difference between the C_{16} isomeric pairs in which the branched-chain compounds afforded greater particle stabilization compared with the linear isomers. In addition, **PEG-G2-bC16** afforded significant stabilization relative to a commercially used PEG-lipid for which the formulation had previously been optimized to enhance storage stability. Thus, in both LNPs from lipid-thiopurine conjugates and the PEG-lipid systems, there is strong preliminary evidence that hydrocarbon branching results in LNP stabilization in buffer. Whether this will translate into enhanced effectiveness in either drug release or transfection will require more detailed cellular studies.

Supplementary material

Supplementary material is available with the article through the journal Web site at http://nrcresearchpress.com/doi/suppl/10.1139/cjc-2016-0462.

Acknowledgements

The ongoing support of the Natural Sciences and Engineering Research Council of Canada is gratefully acknowledged. We thank Precision NanoSystems for their collaborative assistance through the loan of the NanoAssemblr™ and for a gift of their proprietary lipid mixture used in some experiments.

References

(1) Allen, T. M.; Cullis, P. R. *Adv. Drug Delivery Rev.* **2013**, *65*, 36. doi:10.1016/j.addr.2012.09.037.
(2) Tiwari, G.; Tiwari, R.; Sriwastawa, B.; Bhati, L.; Pandey, S.; Pandey, P.; Bannerjee, S. K. *Int. J. Pharm. Invest.* **2012**, *2*, 2. doi:10.4103/2230-973X.96920.
(3) Wicki, A.; Witzigmann, D.; Balasubramanian, V.; Huwyler, J. *J. Controlled Release* **2015**, *200*, 138. doi:10.1016/j.jconrel.2014.12.030.
(4) Petros, R. A.; DeSimone, J. M. *Nat. Rev. Drug Discovery* **2010**, *9*, 615. doi:10.1038/nrd2591.
(5) Das, S.; Chaudhury, A. *AAPS PharmSciTech* **2011**, *12*, 62. doi:10.1208/s12249-010-9563-0.
(6) Koynova, R.; Tenchov, B. *Soft Matter* **2009**, *5*, 3187. doi:10.1039/b902027f.
(7) Semple, S. C.; Akinc, A.; Chen, J.; Sandhu, A. P.; Mui, B. L.; Cho, C. K.; Sah, D. W. Y.; Stebbing, D.; Crosley, E. J.; Yaworski, E.; Hafez, I. M.; Dorkin, J. R.; Qin, J.; Lam, K.; Rajeev, K. G.; Wong, K. F.; Jeffs, L. B.; Nechev, L.; Eisenhardt, M. L.; Jayaraman, M.; Kazem, M.; Maier, M. A.; Srinivasulu, M.; Weinstein, M. J.; Chen, Q.; Alvarez, R.; Barros, S. A.; De, S.; Klimuk, S. K.; Borland, T.; Kosovrasti, V.; Cantley, W. L.; Tam, Y. K.; Manoharan, M.; Ciufolini, M. A.; Tracy, M. A.; de Fougerolles, A.; MacLachlan, I.; Cullis, P. R.; Madden, T. D.; Hope, M. J. *Nat. Biotechnol.* **2010**, *28*, 172. doi:10.1038/nbt.1602.

(8) Wang, T.; Ng, D. Y. W.; Wu, Y.; Thomas, J.; TamTran, T.; Weil, T. *Chem. Commun.* **2014**, *50*, 1116. doi:10.1039/C3CC47003B.
(9) Wang, Y.; Liu, D.; Zheng, Q.; Zhao, Q.; Zhang, H.; Ma, Y.; Fallon, J. K.; Fu, Q.; Haynes, M. T.; Lin, G.; Zhang, R.; Wang, D.; Yang, X.; Zhao, L.; He, Z.; Liu, F. *Nano Lett.* **2014**, *14*, 5577. doi:10.1021/nl502044x.
(10) Israelachvili, J. *Intermolecular and Surface Forces*, 2nd ed.; Academic Press: London, 1992.
(11) Allen, C.; Dos, Santos, N.; Gallagher, R.; Chiu, G. N. C.; Shu, Y.; Li, W. M.; Johnstone, S. A.; Janoff, A. S.; Mayer, L. D.; Webb, M. S.; Bally, M. B. *Biosci. Rep.* **2002**, *22*, 225. doi:10.1023/A:1020186505848.
(12) Leung, A. K. K.; Hafez, I. M.; Baoukina, S.; Belliveau, N. M.; Zhigaltsev, I. V.; Afshinmanesh, E.; Tieleman, D. P.; Hansen, C. L.; Hope, M. J.; Cullis, P. R. *J. Phys. Chem. C* **2012**, *116*, 18440. doi:10.1021/jp303267y.
(13) Heyes, J.; Hall, K.; Tailor, V.; Lenz, R.; MacLachlan, I. *J. Controlled Release* **2006**, *112*, 280. doi:10.1016/j.jconrel.2006.02.012.
(14) Webb, M. S.; Saxon, D.; Wong, F. M. P.; Lim, H. J.; Wang, Z.; Bally, M. B.; Choi, L. S. L.; Cullis, P. R.; Mayer, L. D. *Biochim. Biophys. Acta, Biomembr.* **1998**, *1372*, 272. doi:10.1016/S0005-2736(98)00077-7.
(15) Raetz, C. R. H.; Whitfield, C. *Annu. Rev. Biochem.* **2002**, *71*, 635. doi:10.1146/annurev.biochem.71.110601.135414.
(16) Mehnert, W.; Mäder, K. *Adv. Drug Delivery Rev.* **2012**, *64*, Supplement, 83. doi:10.1016/j.addr.2012.09.021.
(17) Guerbet, M. *C. R. Acad. Sci.* **1909**, *149*, 129.
(18) Matsu-ura, T.; Sakaguchi, S.; Obora, Y.; Ishii, Y. *J. Org. Chem.* **2006**, *71*, 8306. doi:10.1021/jo061400t.
(19) Doura, T.; Yamada, M.; Teranishi, R.; Yamamoto, Y.; Sugimoto, T.; Yuba, E.; Harada, A.; Kono, K. *Langmuir* **2015**, *31*, 5105. doi:10.1021/acs.langmuir.5b00183.
(20) Thota, B. N. S.; Berlepsch, H. v.; Böttcher, C.; Haag, R. *Chem. Commun.* **2015**, *51*, 8648. doi:10.1039/C4CC09513H.
(21) Urakami, C.; Kakeda, K. *Bull. Chem. Soc. Jpn.* **1953**, *26*, 276. doi:10.1246/bcsj.26.276.
(22) Pruett, S. T.; Bushnev, A.; Hagedorn, K.; Adiga, M.; Haynes, C. A.; Sullards, M. C.; Liotta, D. C.; Merrill, A. H. *J. Lipid Res.* **2008**, *49*, 1621. doi:10.1194/jlr.R800012-JLR200.
(23) Kobayashi, H.; Ohashi, J.; Fujita, T.; Iwashita, T.; Nakao, Y.; Matsunaga, S.; Fusetani, N. *J. Org. Chem.* **2007**, *72*, 1218. doi:10.1021/jo062013m.
(24) González, N.; Rodríguez, J.; Jiménez, C. *J. Org. Chem.* **1999**, *64*, 5705. doi:10.1021/jo9903914.
(25) Mitchell, S. S.; Rhodes, D.; Bushman, F. D.; Faulkner, D. J. *Org. Lett.* **2000**, *2*, 1605. doi:10.1021/ol005866o.
(26) Ueoka, R.; Fujita, T.; Iwashita, T.; van Soest, R. W. M.; Matsunaga, S. *Biosci., Biotechnol., Biochem.* **2008**, *72*, 3055. doi:10.1271/bbb.80457.
(27) Ilies, M. A.; Seitz, W. A.; Caproiu, M. T.; Wentz, M.; Garfield, R. E.; Balaban, A. T. *Eur. J. Org. Chem.* **2003**, *2003*, 2645. doi:10.1002/ejoc.200300106.
(28) Niyomtham, N.; Apiratikul, N.; Suksen, K.; Opanasopit, P.; Yingyongnarongkul, B. *Bioorg. Med. Chem. Lett.* **2015**, *25*, 496. doi:10.1016/j.bmcl.2014.12.043.
(29) Zhang, Y.-M.; Chang, D.-C.; Zhang, J.; Liu, Y.-H.; Yu, X.-Q. *Bioorg. Med. Chem.* **2015**, *23*, 5756. doi:10.1016/j.bmc.2015.07.005.
(30) David, S. A.; Silverstein, R.; Amura, C. R.; Kielian, T.; Morrison, D. C. *Antimicrob. Agents Chemother.* **1999**, *43*, 912. PMID:10103199.
(31) Blagbrough, I. S.; Geall, A. J.; David, S. A. *Bioorg. Med. Chem. Lett.* **2000**, *10*, 1959. doi:10.1016/S0960-894X(00)00380-2.
(32) Semple, S. C.; Chonn, A.; Cullis, P. R. *Adv. Drug Delivery Rev.* **1998**, *32*, 3. doi:10.1016/S0169-409X(97)00128-2.
(33) Stanulla, M.; Schaeffeler, E.; Schwab, M. In *Genomics and Pharmacogenomics in Anticancer Drug Development and Clinical Response*; Innocenti, F., Ed.; Humana: New York, 2009; p 173. doi:10.1007/978-1-60327-088-5.
(34) Sahasranaman, S.; Howard, D.; Roy, S. *Eur. J. Clin. Pharmacol.* **2008**, *64*, 753. doi:10.1007/s00228-008-0478-6.
(35) Karran, P.; Attard, N. *Nat. Rev. Cancer* **2008**, *8*, 24. doi:10.1038/nrc2292.
(36) Inamochi, H.; Higashigawa, M.; Shimono, Y.; Nagata, T.; Cao, D.; Mao, X.; M'soka, T.; Hori, H.; Kawasaki, H.; Sakurai, M. *J. Exp. Clin. Cancer Res.* **1999**, *18*, 417.
(37) Wang, J.; Yang, G.; Guo, X.; Tang, Z.; Zhong, Z.; Zhou, S. *Biomaterials* **2014**, *35*, 3080. doi:10.1016/j.biomaterials.2013.12.025.
(38) Jung, D.; Maiti, S.; Lee, J. H.; Lee, J. H.; Kim, J. S. *Chem. Commun.* **2014**, *50*, 3044. doi:10.1039/c3cc49790a.
(39) Wang, J.; Sun, X.; Mao, W.; Sun, W.; Tang, J.; Sui, M.; Shen, Y.; Gu, Z. *Adv. Mater.* **2013**, *25*, 3670. doi:10.1002/adma.201300929.
(40) Vandavasi, J. K.; Hu, W.-P.; Chen, C.-Y.; Wang, J.-J. *Tetrahedron* **2011**, *67*, 8895. doi:10.1016/j.tet.2011.09.071.
(41) McIlhinney, R. A. J.; Harvey, D. J. *J. Mass Spectrom.* **1995**, *30*, 900. doi:10.1002/jms.1190300616.
(42) Belliveau, N. M.; Huft, J.; Lin, P. J. C.; Chen, S.; Leung, A. K. K.; Leaver, T. J.; Wild, A. W.; Lee, J. B.; Taylor, R. J.; Tam, Y. K.; Hansen, C. L.; Cullis, P. R. *Mol. Ther.–Nucleic Acids* **2012**, *1*, e37. doi:10.1038/mtna.2012.28.
(43) Williams, M. S.; Longmuir, K. J.; Yager, P. *Lab Chip* **2008**, *8*, 1121. doi:10.1039/b802562b.
(44) Zhigaltsev, I. V.; Belliveau, N.; Hafez, I.; Leung, A. K. K.; Huft, J.; Hansen, C.; Cullis, P. R. *Langmuir* **2012**, *28*, 3633. doi:10.1021/la204833h.
(45) Song, Y.; Hormes, J.; Kumar, C. S. S. R. *Small* **2008**, *4*, 698. doi:10.1002/smll.200701029.
(46) Delmas, T.; Couffin, A.-C.; Bayle, P. A.; Crécy, F. d.; Neumann, E.; Vinet, F.; Bardet, M.; Bibette, J.; Texier, I. *J. Colloid Interface Sci.* **2011**, *360*, 471. doi:10.1016/j.jcis.2011.04.080.
(47) Hansen, R. E.; Roth, D.; Winther, J. R. *Proc. Natl. Acad. Sci.* **2009**, *106*, 422. doi:10.1073/pnas.0812149106.
(48) Jayaraman, M.; Ansell, S. M.; Mui, B. L.; Tam, Y. K.; Chen, J.; Du, X.; Butler, D.; Eltepu, L.; Matsuda, S.; Narayanannair, J. K.; Rajeev, K. G.; Hafez, I. M.; Akinc, A.; Maier, M. A.; Tracy, M. A.; Cullis, P. R.; Madden, T. D.; Manoharan, M.; Hope, M. J. *Angew. Chem., Int. Ed. Engl.* **2012**, *51*, 8529. doi:10.1002/anie.201203263.
(49) Parvizi, P.; Jubeli, E.; Raju, L.; Khalique, N. A.; Almeer, A.; Allam, H.; Manaa, M. A.; Larsen, H.; Nicholson, D.; Pungente, M. D.; Fyles, T. M. *Int. J. Pharm.* **2014**, *461*, 145. doi:10.1016/j.ijpharm.2013.11.045.
(50) Parvizi-Bahktar, P.; Mendez-Campos, J.; Raju, L.; Khalique, N. A.; Jubeli, E.; Larsen, H.; Nicholson, D.; Pungente, M. D.; Fyles, T. M. *Org. Biomol. Chem.* **2016**, *14*, 3080. doi:10.1039/C6OB00041J.